Choice of high and low thresholds in the rate-based flow control scheme

Y.-C. Lai and Y.-D. Lin

Abstract: In a rate-based flow control scheme, the important issue is how to determine congestion occurrence and congestion relief. The most common method is to set two thresholds of queue length, a high threshold and a low threshold. The values of these two thresholds seriously influence the system performance. Hence the authors present the concept of 'best area' to determine how to set the high and low thresholds to guarantee good performance (i.e. cell loss probability is zero and utilisation is one, if it is possible). Some rules are also given to prevent unnecessary cell loss and under-utilisation, when good performance is not achieved due to too many connections or too large a propagation delay.

1 Introduction

ATM (asynchronous transfer mode) is the most promising transfer technology for implementing B-ISDN. It supports applications with distinct QoS requirements such as delay, jitter, and cell loss and with distinct demands such as bandwidth and throughput. To provide these services for a wide variety of applications, in addition to CBR (constant bit rate), rt-VBR (real-time variable bit rate) and nrt-VBR (non-real-time variable bit rate) service, the ATM forum defined a new service class known as ABR (available bit rate) service to support data applications economically. Also, an end-to-end adaptive control mechanism called closed-loop rate-based flow control is applied to this service. In this control scheme, the allowed cell transmission rate of each ABR connection is dynamically regulated by feedback information from the network [1–6]. If the network is congested, the source end decreases its cell transmission rate when it receives congestion indication. Also, the source end increases its cell transmission rate when congestion is relieved. The rate-based control mechanism can efficiently control the connection flows and utilise the network bandwidth.

Recently several analyses and simulations have been conducted for rate-based flow control schemes. First, Bolot and Shankar used differential equations to model the rate increase and decrease [7]. Yin and Hluchyj proposed analytical models for early versions of ABR control with a timer-based approach [8, 9]. Ramamurthy and Ren developed a detailed analytical model to capture the behaviour of a rate-based flow control scheme and obtain approximate solutions in closed forms [10]. Ohsaki et al. made an analysis and comparison between different switches in the steady state and initial transient state [11–13]. Ritter derived

the closed form expression to quickly estimate the buffer requirements of different switches [14].

These analyses assume that no cell loss occurs at the switch. Based on this assumption, the maximum queue length (buffer requirement) at the switch is derived. However, the switch capacity of a buffer is of finite size, which may be less than the maximum queue length derived. Actually, the maximum queue length ought not to exceed the buffer size at the switch, and extra arrival cells will be lost when the buffer is full. In this paper, we assume the switch capacity of the buffer is finite to reflect real conditions. Also, the performance issues that we are concerned with change from the maximum queue length to cell loss probability and utilisation.

In a rate-based flow control scheme, the common method is to set two thresholds of queue length to determine congestion occurrence and congestion relief. The values of these two thresholds vastly influence the system performance. For example, when the high threshold is large, the switch detects congestion later and thus, cell loss probability would be larger. Similarly, when the low threshold is small, the detection time of congestion relief would be late and cause buffer to underflow and utilisation to drop. Hence some rules, which determine how to set the high and low thresholds, are needed to avoid unnecessary cell loss and under-utilisation.

2 Rate-based flow control

First, we briefly introduce the basic operation of a closed-loop rate-based flow control algorithm [1]. The source end system (SES) sends a forward resource management (RM) cell every N_{rm} data cells to probe the congestion status of the network. The destination end system (DES) returns the forward RM cell as a backward RM cell to the SES. Depending on the received backward RM cell, SES adjusts its allowed cell rate (ACR), which is bounded between peak cell rate (PCR) and minimum cell rate (MCR).

The RM cell contains a 1-bit congestion indication (CI), which is set to zero, and an explicit rate (ER) field which is set to PCR initially by the SES. Depending on the different ways to indicate congestion status, two types of switches are implemented. One is the explicit forward congestion indication (EFCI) the other is the explicit rate (ER) switch.

In the EFCI type, the switch in congestion status sets the EFCI bit to one (EFCI = 1) in the header of each passing data cells. The DES, if a cell with EFCI = 1 has been received, marks the CI bit (CI = 1) to indicate congestion in each backward RM cells. In the ER type, the switch sets the EFCI bit of the RM cells to indicate whether there is congestion or not, and sets the ER field to indicate the bandwidth the VC should use. The performance results and comparisons between two types of switches are shown in [13] in detail.

When the SES receives a backward RM cell, it modifies its ACR using additive increase and multiplicative decrease. The new ACR is computed as follows, depending on CI:

$$ACR = \max(\min(ACR + RIF \cdot PCR, ER), MCR)$$
$$\text{if } CI = 0$$
$$ACR = \max(\min(ACR \cdot (1 - RDF), ER), MCR)$$
$$\text{if } CI = 1$$

where RIF is the rate increase factor and RDF is the rate decrease factor.

In this paper, we focus on the EFCI switch and use a simple model as shown in Fig. 1. There are N_{vc} homogeneous traffic sources sharing a bottleneck link where the bandwidth is BW. We assume that each SES always has cells to send. This assumption allows us to investigate the performance of an EFCI switch in the most stressful situations.
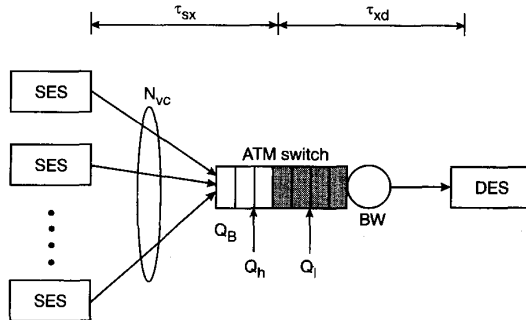

Fig. 1   Analytic model for rate-based flow control

Congestion condition is determined by the switch according to its queue length. There are two values, high threshold Q_h and low threshold Q_l, which decide whether congestion occurs or not. When the queue length exceeds Q_h, the EFCI bit of passing data cells is set to one to indicate congestion. Congestion is relieved when the queue length drops below Q_l.

We define τ_{sx} as the propagation delay between the SES and the switch, and τ_{xd} as the propagation delay between the switch and the DES. Also, the feedback propagation delay from the switch to the SES is denoted by τ_{xds}, and the round trip propagation delay is denoted by τ. Thus we get the relation $\tau_{xds} = \tau_{sx} + 2\tau_{xd}$ and $\tau = 2(\tau_{sx} + \tau_{xd})$. The propagation delay is a critical parameter of system performance.

Note that the buffer at the switch is of finite capacity denoted by Q_B. Due to this fact, the arrival cells shall be lost when the buffer is full. The act of cell loss causes the derivation of the dynamic behaviour of the allowed cell rate, $ACR(t)$, and the buffer size, $Q(t)$, to have some differences with other previous studies.

3   Basic description

We describe the four elementary phases and four different cycles in this Section. A cycle is composed of some elementary phases. Depending on the various compositions of the phases, four different cycles are constructed.

3.1   Elementary phases

The evolution of the ACR can be characterised into four elementary phases differentiated by (i) the increase or decrease of the ACR, and (ii) the speed of the increase or decrease. The speed of adjustment is determined by the rate at which RM cells are received in the SES. Meanwhile, this rate is influenced by the status of the buffer τ_{xds} time units before. So, actually the evolution of the ACR is partitioned into four phases depending on the $ACR(t)$ and $Q(t - \tau_{xds})$.

Phase 1: $ACR(t)$ ↑, $Q(t - \tau_{xds}) > 0$: During this period, each SES receives the backward RM cells with CI = 0 at constant rate $BW/N_{vc}N_{rm}$. When a backward RM cell is received, the SES increases its ACR by $RIF \cdot PCR$, to a rate not greater than PCR. We use a continuous time approximation to model this discrete increase for simplicity. This approximation is accurate to characterise the dynamic behaviour of rate-base control [14]. Thus the following differential equation for $ACR_1(t)$ is given by:

$$\frac{dACR_1(t)}{dt} = \frac{BW \cdot RIF \cdot PCR}{N_{vc}N_{rm}}$$

which gives

$$ACR_1(t)$$
$$= \min\left(ACR_1(0) + \frac{BW \cdot RIF \cdot PCR}{N_{vc}N_{rm}}t, PCR\right) \tag{1}$$

Phase 2: $ACR(t)$ ↓, $Q(t - \tau_{xds}) < Q_B$: During this period, each SES receives the backward RM cells with CI = 1 at constant rate $BW/N_{vc}N_{rm}$. When a backward RM cell is received, the SES reduces its ACR by $ACR \cdot RDF$, to a rate not lower than MCR. We thus have the following continuous approximation for $ACR_2(t)$.

$$\frac{dACR_2(t)}{dt} = -ACR_2(t)\frac{BW \cdot RDF}{N_{vc}N_{rm}}$$

which gives:

$$ACR_2(t) = \max\left(ACR_2(0)e^{-\frac{BW \cdot RDF}{N_{vc}N_{rm}}t}, MCR\right) \tag{2}$$

Phase 3: $ACR(t)$ ↑, $Q(t - \tau_{xds}) = 0$: When the buffer is empty, the switch is not fully utilised. In order not to waste the bandwidth with idle time, we ought to avoid the occurrence of this phase. In this phase, RM cells arrive at the SES depending on its own rate τ time before (i.e. $ACR_3(t - \tau)$). So, the differential equation for $ACR_3(t)$ is given by:

$$\frac{dACR_3(t)}{dt} = ACR_3(t - \tau) \cdot \frac{RIF \cdot PCR}{N_{rm}}$$

which gives:

$$ACR_3(t) = \min\left(ACR_3(0)e^{\beta t}, PCR\right) \tag{3}$$

where β is given as the root of the equation $\beta = (RIF \cdot PCR/N_{rm}) e^{-\beta\tau}$.

Phase 4: $ACR(t)$ ↓, $Q(t - \tau_{xds}) = Q_B$: When the buffer is full, the arrival cells are discarded at the switch. In order not to waste the bandwidth with retransmission of the lost cells, we also hope not to enter this phase. In this phase, although the cell loss happens, RM cells arriving at the SES are still the same as in the previous phase. This is caused by the delay of cells queued in the buffer. After the time Q_B/BW which is the queueing time of cells when the buffer is full, the receiving rate of RM cells at the SES will

change because of the lost cells. For example, if we assume that only data cells can be discarded and RM cells are never lost at the switch, the number of data cells between two consecutive RM cells sent from the same SES are $N_{rm}BW/N_{vc}ACR(t)$, not N_{rm}. That is, after the time Q_B/BW, the rate of the SES receiving the backward RM cells will change from $BW/N_{vc}N_{rm}$ to $ACR(t - Q_B/BW)/N_{rm}$.

In most cases, the interval Q_B/BW is long enough that the change happens after this phase. Hence this change causes the derivation of subsequent phases to be incorrect. Fortunately, data cells and RM cells are both discarded in the switch when the buffer is full. So, the number of data cells between two consecutive RM cells can be approximated as N_{rm}. These approximations show that the derivation of the above phases is still valid. The behaviour of ACR during this phase is given by:

$$\frac{dACR_4(t)}{dt} = -ACR_4(t)\frac{BW \cdot RDF}{N_{vc}N_{rm}}$$

which gives

$$ACR_4(t) = \max\left(ACR_4(0)e^{-\frac{BW \cdot RDF}{N_{vc}N_{rm}}t}, MCR\right) \quad (4)$$

Although the equations of phase 2 and phase 4 are the same, we differentiate between them since there is different meaning.

Note the *MCR* and *PCR* are not considered in the analysis below since we assume $MCR = 0$ and $PCR = BW$. The analysis of $MCR > 0$ or $PCR < BW$ can be expanded from our analysis, but the equations are more complex.

3.2 Various cycles

According to the elementary phases described in the last Subsection, four different cycles are constructed. In all four cycles, phase 1 and phase 2 are the essential phases. The cycles are differentiated by whether phase 3 and phase 4 occur or not.

Best cycle: This perfect cycle is composed of phase 1 and phase 2. They occur alternatively as Fig. 2. When the queue length is below the low threshold (i.e. at the time t_{Q_l}) congestion is relieved in the switch, and this congestion relief signal will arrive at the SES after the propagation delay τ_{xds}. Then the SES increases its *ACR* and phase 1 begins. For convenience in explaining the time shift between $ACR(t)$ and $Q(t)$ caused by the propagation delay, we use the t^+ and t^- to denote the 'after τ_{xds}' and 'before τ_{sx}' time units from the time t, respectively. So, the phase 1 begins at $t_{Q_l}^+$, and similarly, the beginning time of phase 2 is $t_{Q_h}^+$ where t_{Q_h} is the time that queue length exceeds Q_h.
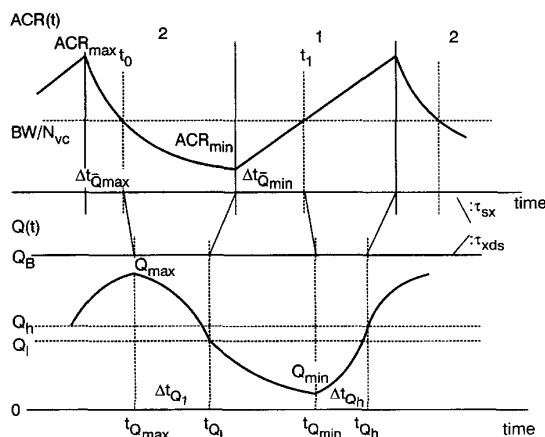

Fig.2 *Evolution of ACR and Q in best cycle*

Let t_0 and t_1 be two time stamps for our analysis. At the time t_0 and t_1, *ACR* is equal to BW/N_{vc}.

Worst cycle: Phase 3 and 4 occurs in this worst case. The cycle behaves as in Fig. 3. In this Figure, phase 4 interrupts phase 2 and phase 3 interrupts phase 1.
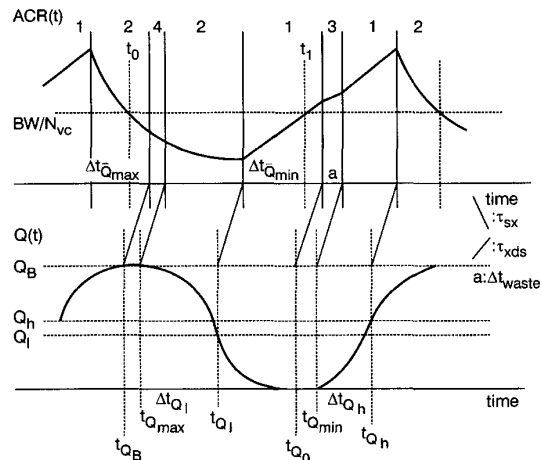

Fig.3 *Evolution of ACR and Q in worst cycle*

When the queue length exceeds Q_B, cell loss starts. Hence phase 4 begins at the $t_{Q_B}^+$, and consequently, the ending time of phase 4 is after τ from t_0. This is because the aggregate cell arrival rate at the switch is below the bandwidth BW at time t_0, and the queue starts to decrease after the propagation delay between the SES and the switch, τ_{sx}. Similarly, the starting time of phase 3 is $t_{Q_0}^+$, where t_{Q_0} is the time that queue length reaches zero, and the ending time of phase 3 is τ time units after the time t_1.

Cell loss cycle: During this cycle, phase 4 occurs and phase 3 does not occur. From Figs. 2 and 3, the sequence of this cycle is phase 1–2–4–2. Also, the beginning time of each phase is obtained in the same way as before.

Under-utilisation cycle: Phase 3 occurs and phase 4 does not occur in this cycle. The sequence of this cycle is phase 1–3–1–2.

4 Choice of high and low thresholds

If we do not carefully choose Q_h and Q_l, not only do the phase 3 and 4 occur, but also the duration of each becomes longer (i.e. more bandwidth is wasted). In this Section, we investigate how to choose the Q_h and Q_l to prevent the system falling into the worst cycle. As shown in Figs. 2 and 3, the evolution of ACR and queue length are deterministic. Hence we can use a differential equation approach to obtain minimum queue length, Q_{min}, maximum queue length, Q_{max}, and cycle time T_{cycle}. Because the derivations are quite complex and trivial, the processes are explained in the Appendix. Note that the derived Q_{max} and Q_{min} are not limited (i.e. the value of Q_{max} might be bigger than the buffer size and the value of Q_{min} might be less than zero).

4.1 Cell loss probability and utilisation

The wasted bandwidth in the cell loss probability and utilisation of four various cycles are calculated as follows.

Best cycle: $Q_{max} \leq Q_B$ and $Q_{min} \geq 0$: In this cycle, the maximum queue length is less than the buffer size in the switch. Also the minimum queue length is larger than zero. In this perfect case, cell loss probability is zero, $P_{loss} = 0$, and utilisation is 1, $\rho = 1$.

Worst cycle: $Q_{max} > Q_B$ and $Q_{min} < 0$: The events of cell loss and under-utilisation occur in this worst case. As we know, when the maximum queue length is larger than the buffer size, the system enters phase 4 and some cells are lost to keep the maximum queue length as buffer size. Similarly, when the minimum queue length is less than zero, the system enters phase 3 and some bandwidth is wasted because of the idle time.

Hence the wasted bandwidth and the number of the lost cells in this cycle are given by:

$$N_{waste} = 0 - Q_{min} \qquad (5)$$

$$N_{loss} = Q_{max} - Q_B \qquad (6)$$

Now utilisation and cell loss probability are:

$$\rho = 1 - \frac{N_{waste}}{T_{cycle} \cdot BW} \qquad (7)$$

$$P_{loss} = \frac{N_{loss}}{T_{cycle} \cdot \rho \cdot BW + N_{loss}} \qquad (8)$$

Cell loss cycle: $Q_{max} > Q_B$ and $Q_{min} \geq 0$: For the cycle where phase 4 occurs and phase 3 does not occur, utilisation is 1, $\rho = 1$, and cell loss probability is directly computed from the worst cases. N_{loss} and P_{loss} are obtained from eqns. 6 and 8.

Under-utilisation cycle: $Q_{max} \leq Q_B$ and $Q_{min} < 0$: For the cycle where phase 3 occurs and phase 4 does not occur, cell loss probability is zero, $P_{loss} = 0$, and utilisation is directly computed from the worst cases. N_{waste} and ρ are obtained from eqns. 5 and 7.

The derivations of P_{loss} and ρ of four various cycles can be integrated by modifying eqns. 5 and 6 to $N_{waste} = \max(0, 0 - Q_{min})$ and $N_{loss} = \max(0, Q_{max} - Q_B)$, respectively. We differentiate them to emphasise the distinction of these cycles.

4.2 Choice of Q_h and Q_l

That Q_{min} is influenced directly by Q_l is obviously observed from above equations. Meanwhile, Q_{min} is also influenced by ACR_{min} which is determined by $\min(Q_B, Q_{max})$. Hence we use the function f to denote the complex expressions. Similarly, let g be the function to calculate Q_{max}.

$$Q_{min} = f(Q_l, \min(Q_B, Q_{max}))$$

$$Q_{max} = g(Q_h, \max(0, Q_{min}))$$

To keep the system operating in the best cycle, we define 'best area' to determine how to set the high and low thresholds. When the point of high and low thresholds is located in the best area, good performance is guaranteed, namely, utilisation is one and cell loss probability is zero. Note the best area may not exist if N_{vc} or τ is large.

First, we get two thresholds Q_l^* and Q_h^* by solving the equation $0 = f(Q_l^*, Q_B)$ and $Q_B = g(Q_h^*, 0)$. The best area can be obtained according to Q_l^* or Q_h^*. None the less, the same best area is obtained whether according to Q_h^* or Q_l^*. Below, we only discuss the solution according to Q_h^*:

Case 1: $Q_h = x \geq Q_h^*$: In this case, Q_{min} must be larger than zero to avoid cell loss (i.e. the expected value Q_{min}^o is the solution of the equation $Q_B = g(x, Q_{min}^o)$). Also, we get Q_l^o by solving $Q_{min}^o = f(Q_l^o, Q_B)$. Therefore, we get the best area ($Q_h = x, Q_l = [Q_l^o, x]$).

Case 2: $Q_h = x < Q_h^*$: In this case, the main concern is to avoid the occurrence of underutilisation. We get Q_{max}^o by solving the equation $Q_{max}^o = g(x, 0)$, and get Q_l^o by solving the equation $0 = f(Q_l^o, Q_{max}^o)$. Therefore, we get the best area ($Q_h = x, Q_l = [Q_l^o, x]$).

Looking at Fig. 4, we partition the space into five areas. If (Q_h, Q_l) is located in the area 'best', the system will operate in the best cycle. If $Q_h > Q_h^*$ and $Q_l < Q_l^*$, that causes $Q_{max} > Q_B$ and $Q_{min} < 0$, the worst cycle occurs. Similarly, areas 'cell loss' and 'under-utilisation' correspond to the cell loss cycle and under-utilisation cycle, respectively. Area 'nonexistence' does not exist because we cannot set $Q_h < Q_l$.
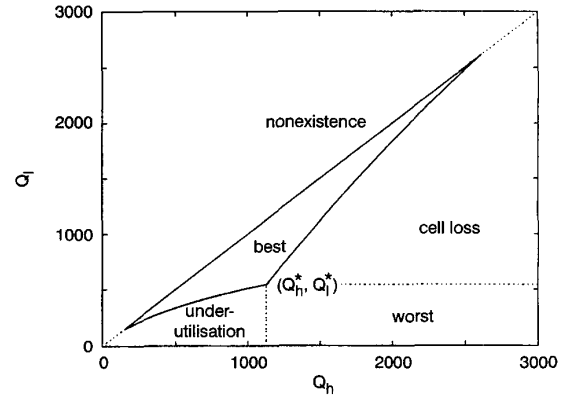

Fig.4 *Five areas to determine Q_h and Q_l*

Rules: (i) When $Q_h^* \geq Q_l^*$, good performance can be achieved. We set (Q_h, Q_l) to locate in the best area. Also to provide more number of connections and larger propagation delay, we ought to set (Q_h, Q_l) to close the centre point of the best area as much as possible. (ii) When $Q_h^* < Q_l^*$, good performance cannot be achieved. When we feel the effect of cell loss is more serious than the effect of under-utilisation, such as loss-sensitive applications, we set ($Q_h = Q_h^*, Q_l = Q_h^*$) to avoid cell loss. (iii) When $Q_h^* < Q_l^*$ and applications are delay-sensitive, we set ($Q_h = Q_l^*, Q_l = Q_l^*$) to avoid under-utilisation.

In a real system, we can create a table of the best areas for the main situations. When the number of sources or the propagation delay changes, the switch can check the table to find the proper values of Q_h and Q_l.

5 Simulation and discussion

Some examples are presented to show the correctness of our analysis of cell loss probability and utilisation. The parameters of the overall systems are set to $N_{vc} = 10$, $BW = 155$Mbps, $PCR = 155$Mbps, $ICR = PCR/20$, $RIF = 1/64$, $RDF = 1/16$, $\tau_{sx}:\tau_{xd} = 1:1$, $\tau = 0.2$ms, $N_{rm} = 32$, $Q_B = 3000$, $Q_h = 2500$, and $Q_l = 500$.

Fig. 5 shows the cell loss probability as a function of the high threshold. There is a good agreement between the analytical and simulation results, which are shown by circles. The small gaps are due to the continuous time approach and the synchronous assumption in the analysis. When Q_h is set too high, P_{loss} increases. This is because the detection time of congestion is too late. Also as N_{vc} becomes larger, cell loss probability is larger. When N_{vc} becomes big, the increase speed of total allowed cell rate, $N_{vc} \cdot ACR$, does not change (i.e. the speed is still $BW \cdot RIF \cdot PCR/N_{rm}$). Hence the maximum total ACR ($N_{vc} \cdot ACR_{max}$) does not change. However, the decrease speed of total ACR slows down. Therefore, cell loss probability increases. When the propagation delay becomes longer, the detection time of congestion between the switch and the sources becomes longer. The slower detection at the sources leads P_{loss} to increase.
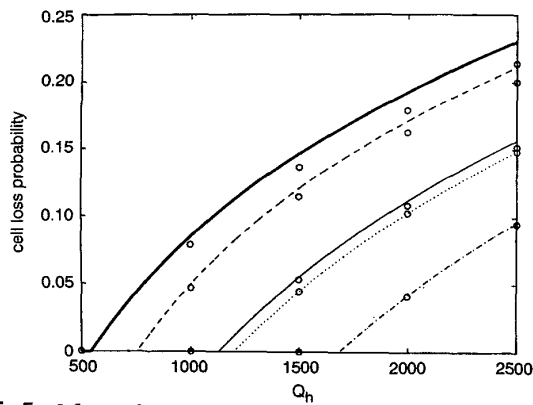
Fig.5 *Influence of Q_h on P_{loss}*
$Q_l = 500$
——————— $N_{vc} = 10$, delay = 0.2ms
············ $N_{vc} = 10$, delay = 0.02ms
━━━━━━ $N_{vc} = 10$, delay = 2ms
·— ·— ·— $N_{vc} = 5$, delay = 0.2ms
— — — — $N_{vc} = 20$, delay = 0.2ms

Actually the value of Q_h not only directly influences Q_{max}, but also indirectly influences Q_{min}. Hence we also observe the influence of Q_h on the utilisation in Fig. 6. In the case with no cell loss, utilisation drops quickly when Q_h increases. However, in the case with cell loss, ρ rises slightly when Q_h increases. As we know, the increment of Q_h directly causes Q_{max} to uprise. In the case with no cell loss, the increment of Q_{max} will cause Q_{min} to drop, with the result that utilisation decreases. But in the case with cell loss, Q_{min} is influenced by Q_B, not by Q_{max}. Hence the wasted bandwidth of under-utilisation does not change. However, the increment of Q_h causes the interval Δt_{Q_h}, which is that the queue length increase from Q_{min} to Q_h, to last longer. Hence the total cycle time is longer and thus, utilisation increases.
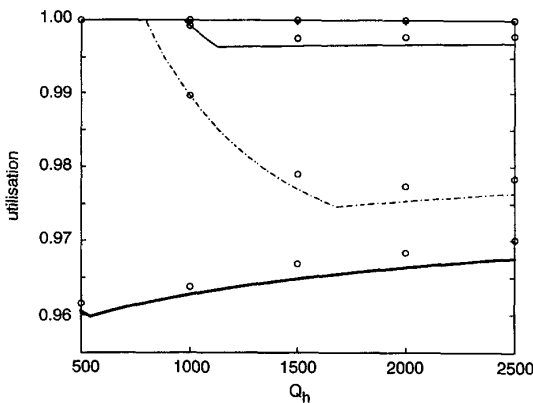

Fig.6 *Influence of Q_h on ρ*
$Q_l = 500$
——————— $N_{vc} = 10$, delay = 0.2ms
············ $N_{vc} = 10$, delay = 0.02ms
━━━━━━ $N_{vc} = 10$, delay = 2ms
·— ·— ·— $N_{vc} = 5$, delay = 0.2ms
— — — — $N_{vc} = 20$, delay = 0.2ms

Note that the case of $N_{vc} = 20$, $\tau = 0.2$ms has no underutilisation. This is because Q_l^* is less than Q_l, which is 500 in this experiment. The similar condition also happens in the case of $N_{vc} = 10$, $\tau = 0.02$ms.

Figs. 7 and 8 show the utilisation and cell loss probability as a function of Q_l, respectively. Again, the analytical and simulation results agree well. The same reasons mentioned above can be applied.

We observe the influence of the number of connections and the round-trip propagation delay, on the best area in
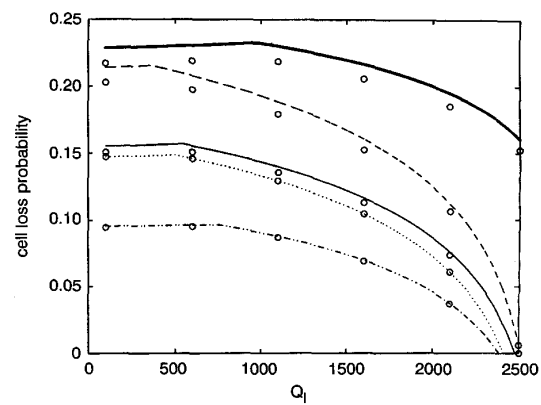

Fig.7 *Influence of Q_l on P_{loss}*
$Q_h = 2500$
——————— $N_{vc} = 10$, delay = 0.2ms
············ $N_{vc} = 10$, delay = 0.02ms
━━━━━━ $N_{vc} = 10$, delay = 2ms
·— ·— ·— $N_{vc} = 5$, delay = 0.2ms
— — — — $N_{vc} = 20$, delay = 0.2ms
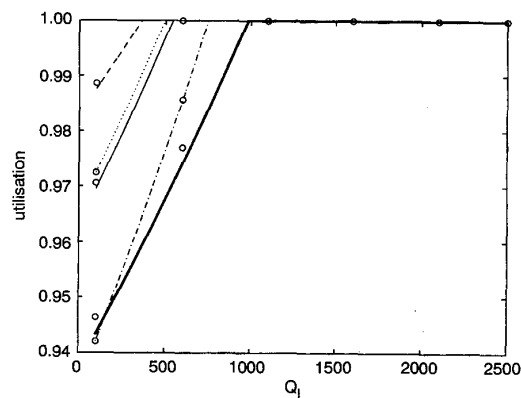
Fig.8 *Influence of Q_l on ρ*
$Q_h = 2500$
——————— $N_{vc} = 10$, delay = 0.2ms
············ $N_{vc} = 10$, delay = 0.02ms
━━━━━━ $N_{vc} = 10$, delay = 2ms
·— ·— ·— $N_{vc} = 5$, delay = 0.2ms
— — — — $N_{vc} = 20$, delay = 0.2ms
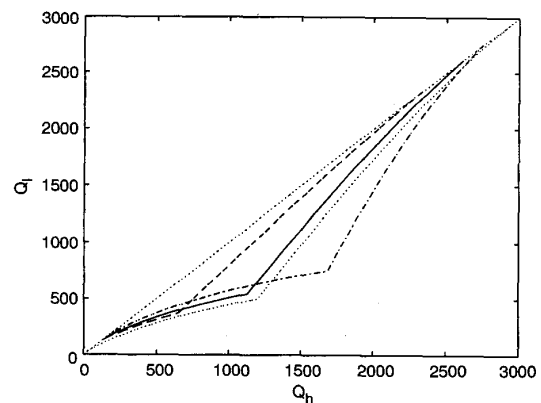
Fig.9 *Comparison of best areas among different N_{vc} and τ*
$Q_h = 2500$
——————— $N_{vc} = 10$, delay = 0.2ms
············ $N_{vc} = 10$, delay = 0.02ms
━━━━━━ $N_{vc} = 10$, delay = 2ms
·— ·— ·— $N_{vc} = 5$, delay = 0.2ms
— — — — $N_{vc} = 20$, delay = 0.2ms

Fig. 9. When N_{vc} becomes large, the best area shrinks, and the centre point of the area slightly drops. The reason is that cell loss probability and utilisation increase when the number of sources increases. Hence Q_h^* and Q_l^* is lower in

the condition of no cell loss and full utilisation. Similarly, when τ becomes large, the best area shrinks. In this case, however, the centre point of the area does not drop. This is caused by the growth of cell loss probability and the reduction of utilisation when the propagation delay becomes large. Note that the best area of $N_{vc} = 10$, $\tau = 2$ms is empty because of $Q_h^* < Q_l^*$.

6 Conclusions and future work

In this paper, an analysis for rate-based flow control is provided. The equations of cell loss probability and utilisation are derived. When the number of sources increases, the cell loss probability increases and utilisation increases. However, when the propagation delay is lengthened, the cell loss probability increases and utilisation decreases.

The concept of 'best area' help us to determine the high and low thresholds. By setting the high and low thresholds in the best area, the system can achieve good performance. When the number of connections becomes larger or the propagation delay becomes longer, the best area shrinks. When the best area shrinks to empty, cell loss or under-utilisation is unavoidable. Nevertheless, rules 2 and 3 are provided to prevent unnecessary cell loss or under-utilisation.

In the future, some directions are also our concerns. First, the generated traffic of sources is usually bursty. The assumption of greedy sources could cause an overestimation of Q_h and Q_l resulting in under-utilisation. Hence the choice of these thresholds under the bursty sources shall be studied. Secondly, the model of a single switch should be expanded into the model of multiple switches. The approach for a multiswitch model is worth developing.

7 References

1 SATHAYE, S.S.: 'Traffic management specification version 4.0'. ATM Forum Contribution 96-tm-0056.000, April 1996
2 CHEN, T.M., LIU, S.S., and SAMALAM, V.K.: 'The available bit rate service for data in ATM networks', *IEEE Commun. Mag.*, 1996, **34**, (5), pp. 56–71
3 FLAVIO, B., and KERRY, W.F.: 'The rate-based flow control framework for the available bit rate ATM service', *IEEE Netw.*, 1995, **9**, (2), pp. 25–39
4 LAI, Y.C., and LIN, Y.D.: 'Interoperability of EFCI and ER switches for ABR services in ATM networks', *IEEE Netw.*, 1998, **12**, (1), pp. 34–43
5 CHARNY, A., RAMAKRISHNAN, K.K., and LAUCK, A.: 'Time scale analysis and scalability issues for explicit rate allocation in ATM networks', *IEEE/ACM Trans. Netw.*, 1996, **4**, (4), pp. 569–581
6 ALTMAN, E., BASAR, T., and SRIKANT, R.: 'Robust rate control for ABR sources'. Proceedings of IEEE INFOCOM'98, San Francisco, 1998
7 BOLOT, J.C., and SHANKAR, A.U.: 'Dynamical behaviour of rate-based flow control mechanisms', *Comput. Commun. Rev.*, 1990, **20**, (2), pp. 35–49
8 YIN, N., and HLUCHYJ, M.G.: 'On close-loop rate control for ATM cell relay networks'. Proceedings of IEEE INFO-COM'94, Toronto, 1994, pp. 99–108
9 YIN, N.: 'Analysis of a rate-based traffic management mechanism for ABR service'. Proceedings of IEEE GLOBECOM'95, Singapore, 1995, pp. 1076–1082
10 RAMAMURTHY, G., and REN, Q.: 'Analysis of the adaptive rate control for ABR service in ATM networks'. Proceedings of IEEE GLOBECOM'95, Singapore, 1995, pp. 1083–1088
11 OHSAKI, H., MURATA, M., SUZUKI, H., IKEDA, C., and MIYAHARA, H.: 'Analysis of rate-based congestion control algorithms for ATM networks, Part 1: Steady state analysis'. Proceedings of IEEE GLOBECOM'95, Singapore, 1995, pp. 296–303
12 OHSAKI, H., MURATA, M., SUZUKI, H., IKEDA, C., and MIYAHARA, H.: 'Analysis of rate-based congestion control algorithms for ATM networks, Part 2: Initial transient state analysis'. Proceedings of IEEE GLOBECOM'95, Singapore, 1995, pp. 1095–1101
13 OHSAKI, H., MURATA, M., SUZUKI, H., IKEDA, C., and MIYAHARA, H.: 'Rate-based congestion control for ATM networks', *Comput. Commun. Rev.*, 1995, **25**, (2), pp. 60–72
14 RITTER, M.: 'Network buffer requirement of the rate-based control mechanism for ABR services'. Proceedings of IEEE INFOCOM'96, San Francisco, 1996, pp. 1190–1197

8 Appendix

Depending on which phase the time marking is located in, different cases should be considered. For example, t_{Q_0} can be in phase 1 or phase 2, and t_{Q_h} can be in phase 3 or phase 1. However, when we carefully set the Q_h and Q_l according to the rules described in the section 4, the time between t_{Q_l} and t_{Q_0} is long and the duration of phase 3 is short. Therefore, most situations shall be the case shown as Figs. 2 and 3. Due to a lack of space, we will only derive the equations of the cases in Figs. 2 and 3.

At time t_0, the aggregate cell arrival rate at the switch is below bandwidth, BW, and queue starts to decrease after the propagation delay between the SES and the switch, τ_{sx}. After the time Δt_{Q_l}, the buffer content reaches the low threshold, Q_l, and the ACR at the SES stops decreasing at $t_{Q_l}^+$. Although this period crosses phase 2 and phase 4, the same dynamic behaviour exists for phase 2 and phase 4. Thus we have

$$\int_0^{\Delta t_{Q_l}} BW\left(1 - e^{-\frac{BW \cdot RDF}{N_{vc} N_{rm}} t}\right) dt = \min(Q_{max}, Q_B) - Q_l$$

Hence the time interval Δt_{Q_l} is got as the root of:

$$BW \cdot \Delta t_{Q_l} + \frac{N_{vc} N_{rm}}{RDF} \cdot e^{-\frac{BW \cdot RDF}{N_{vc} N_{rm}} \Delta t_{Q_l}}$$
$$= \min(Q_{max}, Q_B) - Q_l + \frac{N_{vc} N_{rm}}{RDF}$$

The minimum rate, ACR_{min}, is given by:

$$ACR_{min} = \frac{BW}{N_{vc}} e^{-\frac{BW \cdot RDF}{N_{vc} N_{rm}}(\Delta t_{Q_l} + \tau)}$$

Let $ACR_{t_0}(t)$ be the evolution of the ACR from time t_0, which is given by:

$$ACR_{t_0}(t) = \frac{BW}{N_{vc}} e^{-\frac{BW \cdot RDF}{N_{vc} N_{rm}} t}$$

At the time that the ACR becomes minimum, the SES begins to increase its ACR and the system enters phase 1. After the time $\Delta t_{Q_{min}}^-$ the aggregate cell arrival at the switch is over BW. Hence we get:

$$\Delta t_{Q_{min}}^- = \frac{N_{rm}(BW - N_{vc} \cdot ACR_{min})}{BW \cdot RIF \cdot PCR}$$

Now the minimum queue length, Q_{min}, is given by:

$$Q_{min} = \min(Q_{max}, Q_B)$$
$$- \int_0^{\Delta t_{Q_l} + \tau} (BW - N_{vc} \cdot ACR_{t_0}(t)) \, dt$$
$$- \int_0^{\Delta t_{Q_{min}}^-} (BW - N_{vc} \cdot ACR_1(t)) \, dt$$

Using $ACR_1(0) = ACR_{min}$, Δt_{Q_l}, $\Delta t_{Q_{min}}^-$, and $ACR_{t_0}(t)$ from the above equations, finally we have:

$$Q_{min} = Q_l - \tau \cdot BW$$
$$+ \frac{N_{vc} N_{rm}}{RDF} \cdot e^{-\frac{BW \cdot RDF}{N_{vc} N_{rm}} \Delta t_{Q_l}} \cdot \left(1 - e^{-\frac{BW \cdot RDF}{N_{vc} N_{rm}} \cdot \tau}\right)$$
$$- \frac{N_{rm}(BW - N_{vc} \cdot ACR_{min})^2}{2 \cdot BW \cdot RIF \cdot PCR}$$

$$(9)$$

If Q_{min} is larger than zero, phase 3 does not occur, and no bandwidth is wasted. On the other hand, if Q_{min} is less than

zero, phase 3 occurs. Below we consider two cases according to whether phase 3 occurs or not.

Case 1: phase 3 does not occur

First, we get the equation of the interval Δt_{Q_h}, which is the time that the queue length increases from Qmin to Q_h. Since the increasing rate of ACR at each SES is $(BW \cdot RIF \cdot PCR)/(N_{vc} \cdot N_{rm})$ from eqn. 1, we get:

$$\Delta t_{Q_h} = \sqrt{\frac{2N_{rm}(Q_h - Q_{min})}{BW \cdot RIF \cdot PCR}}$$

The maximum rate, ACR_{max} is given by:

$$ACR_{max} = \frac{BW}{N_{vc}} \left(1 + \frac{RIF \cdot PCR}{N_{rm}} \cdot (\tau + \Delta t_{Q_h}) \right)$$

At the time that the ACR becomes maximum, the SES begins to decrease its ACR and the system enters phase 2. After the time $\Delta t_{Q_{max}}^-$, the aggregate cell arrival at the switch is below BW, and the queue length begins to decrease. So we have:

$$ACR_{max}e^{-\frac{BW \cdot RDF}{N_{vc}N_{rm}}\Delta t_{Q_{max}}^-} = BW/N_{vc}$$

which is solved as:

$$\Delta t_{Q_{max}}^- = -\frac{N_{vc}N_{rm}}{BW \cdot RDF} \log \frac{BW}{N_{vc} \cdot ACR_{max}}$$

Now the maximum queue length, Q_{max}, is given by:

$$Q_{max} = Q_{min} + \int_0^{\Delta t_{Q_h}+\tau} \left(\frac{BW \cdot RIF \cdot PCR}{N_{rm}} \cdot t \right) dt$$

$$+ \int_0^{\Delta t_{Q_{max}}^-} (N_{vc} \cdot ACR_2(t) - BW)dt$$

Using $ACR_2(0) = ACR_{max}$, Δt_{Q_h}, $\Delta t_{Q_{max}}^-$ and $ACR_2(t)$ from above equation, finally we have:

$$Q_{max} = Q_h$$
$$+ \tau \cdot \sqrt{\frac{2(Q_h - Q_{min}) \cdot BW \cdot RIF \cdot PCR}{N_{rm}}}$$
$$+ \frac{\tau^2 \cdot BW \cdot RIF \cdot PCR}{2N_{rm}}$$
$$+ \frac{N_{vc}N_{rm}}{RDF} \left(\log \left(\frac{BW}{N_{vc} \cdot ACR_{max}} \right) \right.$$
$$\left. + \frac{N_{vc} \cdot ACR_{max}}{BW} - 1 \right) \tag{10}$$

Case 2: phase 3 occurs

To obtain the ACR_{max} in this case, first we compute the length of phase 3, Δt_{waste}, as:

$$\Delta t_{waste} = \Delta t_{Q_{min}}^- - \Delta t_{Q_0}^-$$

where $\Delta t_{Q_0}^-$ is the interval between the time of the minimum rate and the time t_{Q_0}. We get $\Delta t_{Q_0}^-$ by solving the equation,

$$0 = \min(Q_B, Q_{max})$$
$$- \int_0^{\Delta t_{Q_l}+\tau} (BW - N_{vc} \cdot ACR_{t_0}(t))dt$$
$$- \int_0^{\Delta t_{Q_0}^-} (BW - N_{vc} \cdot ACR_1(t))dt$$

Now we calculate the ACR_{max}:

$$ACR_3(0) = \frac{BW}{N_{vc}} + \frac{BW \cdot RIF \cdot PCR}{N_{vc}N_{rm}}(\tau - \Delta t_{waste})$$
in phase 1

$$ACR_1(0) = ACR_3(0)e^{\beta \Delta t_{waste}}$$ in phase 3

$$ACR_{Q_h}^- = ACR_1(0) + \frac{BW \cdot RIF \cdot PCR}{N_{vc}N_{rm}}\Delta t_{Q_h}^-$$
in phase 1

$$ACR_{max} = ACR_{t_{Q_h}}^- + \frac{BW \cdot RIF \cdot PCR}{N_{vc}N_{rm}}\tau$$
in phase 1

where $\Delta t_{Q_h}^-$ is the interval between the beginning time of phase 1 and the time t_{Q_h}. We get $\Delta t_{Q_h}^-$ by solving the equation,

$$Q_h = \int_0^{\tau - \Delta t_{waste}} \frac{BW \cdot RIF \cdot PCR}{N_{rm}} \cdot tdt$$
$$+ \int_0^{\Delta t_{waste}} (N_{vc}ACR_3(0)e^{\beta t} - BW)dt$$
$$+ \int_0^{\Delta t_{Q_h}^-} \left(N_{vc}\left(ACR_1(0) + \frac{BW \cdot RIF \cdot PCR}{N_{vc}N_{rm}}t \right) \right.$$
$$\left. - BW \right) dt$$

The maximum queue length is obtained as:

$$Q_{max} = Q_h + \int_0^{\tau} \left(N_{vc}\left(ACR_{Q_h}^- \right.\right.$$
$$\left.\left. + \frac{BW \cdot RIF \cdot PCR}{N_{vc}N_{rm}}t \right) - BW \right) dt$$
$$+ \int_0^{\Delta t_{Q_{max}}^-} (N_{vc} \cdot ACR_2(t) - BW) dt \tag{11}$$

Now we get the cycle time T_{cycle} as:

$$T_{cycle} = 2\tau + \Delta t_{Q_l} + \Delta t_{Q_{min}}^- + \Delta t_{Q_h} + \Delta t_{Q_{max}}^- \tag{12}$$